

A Study of C–F···M⁺ Interaction: Alkali Metal Complexes of the Fluorine-Containing Cage Compound

Hiroyuki Takemura,^{*,†} Noriyoshi Kon,[‡] Masayuki Kotoku,[‡] Sachiko Nakashima,[‡] Kazuhiro Otsuka,[‡] Mikio Yasutake,[§] Teruo Shinmyozu,[§] and Takahiko Inazu[‡]

Department of Chemistry, Faculty of Science, Kyushu University, Ropponmatsu 4-2-1, Chuo-ku, Fukuoka 810-8560, Japan, Department of Chemistry, Faculty of Science, Kyushu University, Hakozaki 6-10-1, Higashi-ku, Fukuoka 812-8581, Japan, and Institute for Fundamental Research of Organic Chemistry, Kyushu University, Hakozaki 6-10-1, Higashi-ku, Fukuoka 812-8581, Japan

takemura@rc.kyushu-u.ac.jp

Received November 29, 2000

The C–F···M⁺ interaction was investigated by employing a cage compound **1** that has four fluorobenzene units. The NMR (¹H, ¹³C, and ¹⁹F) spectra and X-ray crystallographic analyses of **1** and its metal complexes showed clear evidence of the interaction. Short C–F···M⁺ distances (C–F···K⁺, 2.755 and 2.727 Å; C–F···Cs⁺, 2.944 and 2.954 Å) were observed in the crystalline state of K⁺ ⊂ **1** and Cs⁺ ⊂ **1**. Furthermore, the C–F bond lengths were elongated by the interaction with the metal cations. By calculating Brown's bond valence, it is shown that the contribution of the C–F unit to cation binding is comparable or greater than the ether oxygen in the crystalline state. Representative spectroscopic changes implying the C–F···M⁺ interaction were observed in the NMR (¹H, ¹³C, and ¹⁹F) spectra. In particular, ¹³Cs–¹⁹F spin coupling (*J* = 54.9 Hz) was observed in the Cs⁺ complex.

Introduction

On the basis of recent research, it has become apparent that the fluorine atom covalently bonded to a carbon atom acts as a donor unit to cations (Figure 1).¹ In previous papers, we revealed that the C–F unit binds alkali metal cations, NH₄⁺, and Ag⁺ by employing the hexafluoro cage compound **4** (Figure 2).² We showed the first example of a host–guest complex system in which metal cations are captured only by the C–F unit. As shown in the series of fluorinated macrocyclic compounds, preorganization of the C–F unit for cations is the most important factor for capturing spherical metal cations.^{2b} Characteristic NMR spectroscopic changes (¹H, ¹³C, and ¹⁹F) were observed as a result of the C–F···M⁺ interaction. We also confirmed that the C–F bond lengths of the complexes (K⁺ and NH₄⁺ ⊂ **4**) were longer than that of the metal-free **4** in the crystalline structures.

On the other hand, we reported the cation and anion inclusion ability of the cage compound **3**, which consists of four pyridine rings and two ethyleneoxa units.³ This compound has a strong cation affinity because it has eight nitrogen atoms and two oxygen atoms as donors in its cavity, and thus, a total of 20 electrons are converged



Figure 1. Schematic illustration of the C–F···M⁺ interaction.

into the cavity. Therefore, by the replacement of four pyridine rings with a fluorobenzene unit, we can expect to observe the C–F···M⁺ interaction by this new host molecule. Furthermore, different from compound **4**, we can simultaneously compare the contribution of the binding power of C–F···M⁺, –O···M⁺, and =N···M⁺. In this paper, estimation of the C–F···M⁺ interaction is described by measurement of the stability constants, the ¹H, ¹³C, and ¹⁹F NMR spectral features, and X-ray crystallographic analyses of M⁺ ⊂ **1**.

Results and Discussion

Coordination Structures of K⁺ ⊂ **1** and Cs⁺ ⊂ **1**.

The cage compounds described in this paper were synthesized by the one-step coupling procedure previously described (Figure 2).⁴ Compound **1** was obtained as a potassium complex, K⁺ ⊂ **1**, while the fluorine-free compound **2** was obtained as the metal-free form. Since basic molecular skeletons of both compounds are regarded as the same, it is obvious that the C–F unit has a donor ability to metal cations. Here, we have to remember that Plenio et al. reported a very similar compound that consists of two diethyleneoxa units and four fluorobenzene units. They reported very short C–F···Cs⁺ distances in the cesium complex and concluded that

(4) (a) Kon, N.; Takemura, H.; Otsuka, K.; Tanoue, K.; Nakashima, S.; Yasutake, M.; Tani, K.; Kimoto, J.; Shinmyozu, T.; Inazu, T. *J. Org. Chem.* **2000**, *65*, 3708–3715. (b) Takemura, H.; Inazu, T. *J. Synth. Org. Chem. Jpn.* **1998**, *56*, 604–614. (c) Takemura, H.; Shinmyozu, T.; Inazu, T. *Coord. Chem. Rev.* **1996**, *156*, 183–200.

* To whom correspondence should be addressed. Tel: +81-92-726-4755. Fax: +81-92-726-4755.

[†] Kyushu University, Ropponmatsu.

[‡] Kyushu University, Hakozaki.

[§] Institute for Fundamental Research of Organic Chemistry.

(1) Plenio, H. *Chem. Rev.* **1997**, *97*, 3363–3384 and references therein.

(2) (a) Takemura, H.; Kon, N.; Yasutake, M.; Kariyazono, H.; Shinmyozu, T.; Inazu, T. *Angew. Chem.* **1999**, *111*, 1012–1014; *Angew. Chem., Int. Ed. Engl.* **1999**, *38*, 959–961. (b) Takemura, H.; Kariyazono, H.; Yasutake, M.; Kon, N.; Tani, K.; Sako, K.; Shinmyozu, T.; Inazu, T. *Eur. J. Org. Chem.* **2000**, 141–148. (c) Takemura, H.; Kon, N.; Yasutake, M.; Nakashima, S.; Shinmyozu, T.; Inazu, T. *Chem. Eur. J.* **2000**, *6*, 2334–2337.

(3) Takemura, H.; Otsuka, K.; Kon, N.; Yasutake, M.; Shinmyozu, T.; Inazu, T. *Tetrahedron Lett.* **1999**, *40*, 5561–5564.

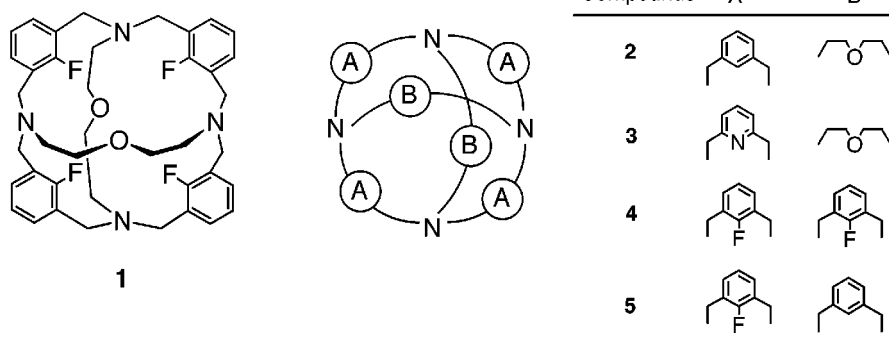


Figure 2. Structures of the tetrafluoro cage compound **1** and its derivatives.

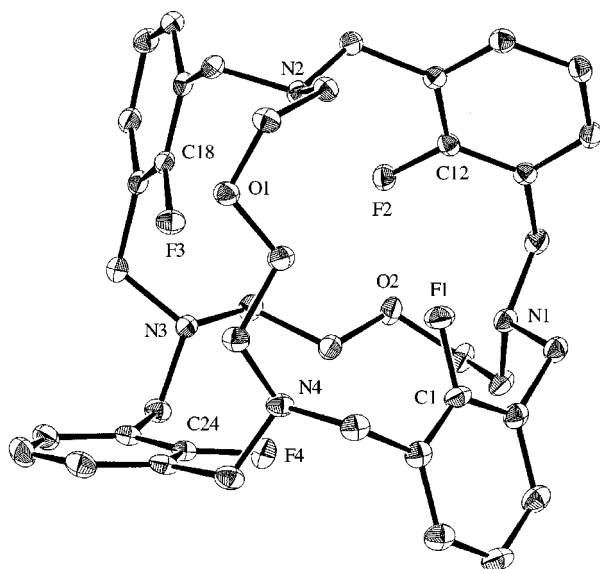


Figure 3. X-ray crystallographic structure of **1** (H atoms are omitted for clarity). Bond lengths (Å): C1–F1, 1.358(2); C12–F2, 1.355(2); C18–F3, 1.355(2); C24–F4, 1.356(2).

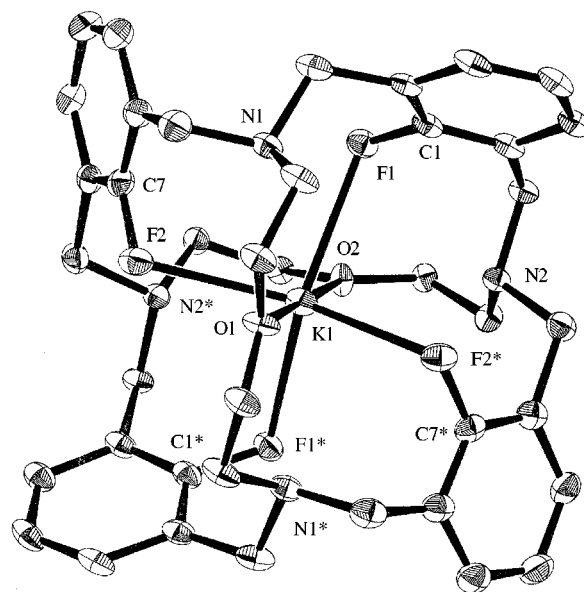


Figure 4. X-ray crystallographic structure of K⁺ \subset **1** (H atoms are omitted for clarity).

contribution of the C–F unit to stabilization of the cation is superior to the ether oxygen in their complex.⁵

In this research, we chose alkali metal cations in order to investigate the C–F \cdots M⁺ interaction. This is because the cations have a wide range of ionic radii, and the effect of the *d* electrons can be ignored when C–F units interact with them. Therefore, these are suitable metal cations for estimating the C–F \cdots M⁺ interaction on the basis of charge and ionic radii.

X-ray crystallographic analysis plays an important role in proving the interaction between C–F and cations. Figures 3–5 show the structures of the metal-free **1**, K⁺ \subset **1**, and Cs⁺ \subset **1**, respectively. In the metal-free **1**, two oxygen atoms are directed outward from the molecular cavity, while the lone pairs of the oxygen in K⁺ \subset **1** and Cs⁺ \subset **1** are directed to the metal cation center: structural changes occur so as to stabilize the cation-inclusion form.

Here, three requirements are desired as proof of the C–F \cdots M⁺ interaction: (1) the C–F bond length becomes longer by the interaction, (2) a short C–F \cdots M⁺ distance is observed, and the third requirement is described below.

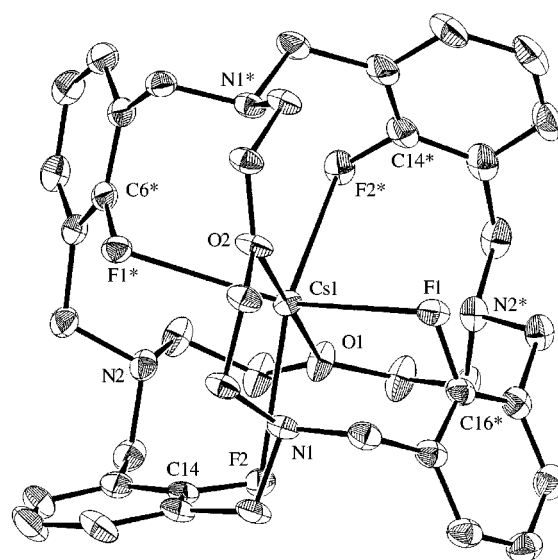


Figure 5. X-ray crystallographic structure of Cs⁺ \subset **1** (H atoms are omitted for clarity).

The average C–F bond lengths of metal-free **1** is 1.356 Å, while those of the K⁺ \subset **1** and Cs⁺ \subset **1** are 1.382 and 1.369 Å, respectively (Tables 1 and 2). Obviously, the

(5) Plenio, H.; Diodone, R.; Badura, D. *Angew. Chem.* **1997**, *109*, 130–132; *Angew. Chem., Int. Ed. Engl.* **1997**, *36*, 156–158.

Table 1. Representative Bond Lengths, Interatomic Distances, and Bond Angles of $K^+ \subset \mathbf{1}$

bond lengths (Å)		interatomic distances (Å)		bond angles (deg)	
C1–F1	1.380(5)	F1...K1	2.755(3)	C1–F1...K1	108.8(2)
C7–F2	1.383(6)	F2...K1	2.727(3)	C7–F2...K1	107.4(2)
		O1...K1	3.034(5)	O1–K1...O2	180.0
		O2...K1	3.081(4)	F1–K1...F1*	134.8(1)
		N1...K1	3.310(4)	F2–K1...F2*	136.5(1)
		N2...K1	3.370(4)		

Table 2. Representative Bond Lengths, Interatomic Distances, and Bond Angles of $Cs^+ \subset \mathbf{1}$

bond lengths (Å)		interatomic distances (Å)		bond angles (deg)	
C6–F1	1.369(3)	F1...Cs1	2.944(2)	C6–F1...Cs1	101.5(1)
C14–F2	1.368(3)	F2...Cs1	2.954(2)	C14–F2...Cs1	101.8(1)
		O1...Cs1	3.094(2)	O1–Cs1...O2	180.0
		O2...Cs1	3.075(2)	F1–Cs1...F1*	132.12(6)
		N1...Cs1	3.365(2)	F2–Cs1...F2*	133.29(6)
		N2...Cs1	3.344(2)		

C–F bonds are elongated by the interaction. The changes of the lengths are small, but these are not caused by experimental errors or by libration of thermal ellipsoids. That was observed in every case of our complexes, i.e., $NH_4^+ \subset \mathbf{4}$, $K^+ \subset \mathbf{4}$,² and other examples ($Tl^+ \subset \mathbf{4}$ and $La^{3+} \subset \mathbf{1}$) which were recently observed. The $K^+ \cdots F$ distances are 2.755 and 2.727 Å, which are the shortest next to that of $K^+ \subset \mathbf{4}$ (2.563 Å).^{1,2a} On the other hand, the $K^+ \cdots O$ distances are 3.034 and 3.081 Å. Considering that the $K^+ \cdots O$ distances in $K^+ \subset 18$ -crown-6 are 2.77–2.83 Å,⁶ bonding of the oxygen to the cation center is weak in $K^+ \subset \mathbf{1}$. The $K^+ \cdots N$ distances are also long (3.310 and 3.370 Å), and the contribution can also be regarded as very small. Considering that the sum of the van der Waals radii of the oxygen and nitrogen atoms and ionic radius of K^+ are 2.85 and 2.88 Å, respectively, the interactions of $K^+ \cdots O$ and $K^+ \cdots N$ are weak in this case.

In the case of $Cs^+ \subset \mathbf{1}$, the interatomic distances $Cs^+ \cdots F = 2.944$ and 2.954 Å are the shortest next to the example of Plenio et al. (2.843 and 3.047 Å).⁵ The $Cs^+ \cdots O$ distances of $Cs^+ \subset \mathbf{1}$ are 3.094 and 3.075 Å, which are longer than the $Cs^+ \cdots F$ distances but shorter than that of the $Cs^+ \subset 18$ -crown-6 complex (3.15 Å in average).⁷ The $Cs^+ \cdots N$ distances are long (3.365 and 3.344 Å), and thus, bonds between the N atoms and Cs^+ can be considered as weak. We have already shown that the bridgehead nitrogen atoms are not a concern in the binding of the metal cations in the case of analogues of cage compound $\mathbf{1}$.²

The contribution of each ligand to cation bonding can be estimated using Brown's bond-valence calculation.⁸ Two research groups employed this method in order to evaluate the C–F...M⁺ bonding.^{5,9} Bond valences, s , of $K^+ \subset \mathbf{1}$ and $Cs^+ \subset \mathbf{1}$ were calculated on the basis of their X-ray crystallographic data. As a result, $\sum s(K \cdots F) = 0.620$, $\sum s(K \cdots O) = 0.178$, $\sum s(K \cdots N) = 0.212$ ($V = \sum s = 1.01$); $\sum s(Cs \cdots F) = 0.689$, $\sum s(Cs \cdots O) = 0.329$, $\sum s(Cs \cdots N)$

$= 0.395$ ($V = 1.41$) were obtained.¹⁰ In the case of $Cs^+ \subset \mathbf{1}$, the sum of s values becomes considerably greater than 1.00. This is because the cavity size of $\mathbf{1}$ is not so variable while cesium has a large ionic radius. Because the s value is a function of r (ligand–cation distances), the s becomes large when the relative distances between Cs^+ and F, N, and O are short. However, this deviation does not affect the estimation of the bonding contribution of each ligand to Cs^+ . On the basis of these values, it is concluded that C–F...M⁺ bonding is dominant ($s = 0.155$ per one C–F...K⁺, 0.0890 per one O...K⁺, and 0.0530 per one N...K⁺) in $K^+ \subset \mathbf{1}$, and in the case of $Cs^+ \subset \mathbf{1}$, contribution of C–F...Cs⁺ and O...Cs⁺ is comparable ($s = 0.172$ per one C–F...Cs⁺, 0.165 per one O...Cs⁺, and 0.0988 per one N...Cs⁺).

A dominant factor in the C–F...M⁺ interaction can be considered as a cation–dipole interaction rather than a coordination bond. The dative bond of the F atom to cation is considered to be smaller than that of the oxygen or nitrogen atom because the ionization potential of the F atom is larger than that of the O or N atom. The cation–dipole interaction between fluorobenzene and M⁺ is larger than that of the ether oxygen or amine nitrogen. Because each donor unit of the compound $\mathbf{1}$ is regarded as fluorobenzene, diethyl ether, and triethylamine, respectively, this is recognized by the comparison of the dipole moment, i.e., fluorobenzene, 1.61; diethyl ether, 1.15; and triethylamine, 0.77.¹¹ The cation–dipole interaction is dominant especially in the binding of alkali metal cations because they do not have d orbitals available for the dative bond like transition metals.

The interaction is roughly estimated by a simple equation as follows

$$E = -Q\mu \cos \theta / 4\pi\epsilon r^2$$

where μ = dipole moment, θ = C–F...M⁺ (O...M⁺) angle, ϵ = permittivity, and r = interatomic distance. If we put the data of X-ray analysis of $Cs^+ \subset \mathbf{1}$ into the equation, each stabilization energy E (sum of four C–F...Cs⁺ and two O...Cs⁺) was obtained as follows. $E(C-F \cdots Cs^+) = 1.9$ kcal mol⁻¹ and $E(O \cdots Cs^+) = 3.1$ kcal mol⁻¹ in fluorobenzene, respectively. The sum of the stabilization energy is 5.0 kcal mol⁻¹, which is almost equal to the free energy, $\Delta G = 3.7$ – 4.3 kcal mol⁻¹, estimated by the binding constants K_s described below. Although the cation–dipole interaction strongly depends on the angle, the C–F...M⁺ interaction operates in enough strength even if the angles are around 100° (Table 2).

Complexation Studies. The stability constants of M⁺ $\subset \mathbf{1}$ were estimated by employing metal-free $\mathbf{1}$ and alkali metal picrates. Since compound $\mathbf{1}$ was obtained as a potassium complex, K⁺ was removed by dissolving the complex in aqueous HCl. The metal-free $\mathbf{1}$ was precipitated from the aqueous solution of the hydrochloride by aqueous Me₄NOH treatment. The reactions between $\mathbf{1}$ and metal picrates were monitored by the ¹H NMR

(6) Seiler, P.; Dobler, M.; Dunitz, J. D. *Acta Crystallogr.* **1974**, *B30*, 2744–2745.

(7) Dobler, M.; Phizackerley, R. P. *Acta Crystallogr.* **1974**, *B30*, 2748–2750.

(8) (a) Brown, I. D.; Altermatt, D. *Acta Crystallogr.* **1985**, *B41*, 244–247. (b) Brown, I. D.; Wu, K. K. *Acta Crystallogr.* **1976**, *B32*, 1957–1959. (c) Brown, I. D.; Shannon, R. D. *Acta Crystallogr.* **1973**, *A29*, 266–282.

(9) Murray-Rust, P.; Stallings, W. C.; Monti, C. T.; Preston, R. K.; Glusker, J. P. *J. Am. Chem. Soc.* **1983**, *105*, 3206–3214.

(10) Bond-valence sum was calculated according to ref 8a: $s = \exp[-(r_0 - r)/B]$, $B = 0.37$. The value r_0 was calculated using the equation, $r_0 = r_c + A \times r_a + P - D - F$. In the case of the K⁺ complex, the best result (total sum of s approaches 1.00) was obtained by employing the calculated r_0 rather than the experimental one. The values $r_0 = 2.051$ for K–F, 2.161 for K–O, 2.251 for K–N were employed for the calculation. In the case of the Cs⁺ complex, the experimental r_0 value was well reproduced by the calculation employing $D = 0.1$. The values $r_0 = 2.298$ for Cs–F, 2.417 for Cs–O, and 2.498 for Cs–N were employed for the calculation.

(11) *Lange's Handbook of Chemistry*; McGraw-Hill: New York, 1985.

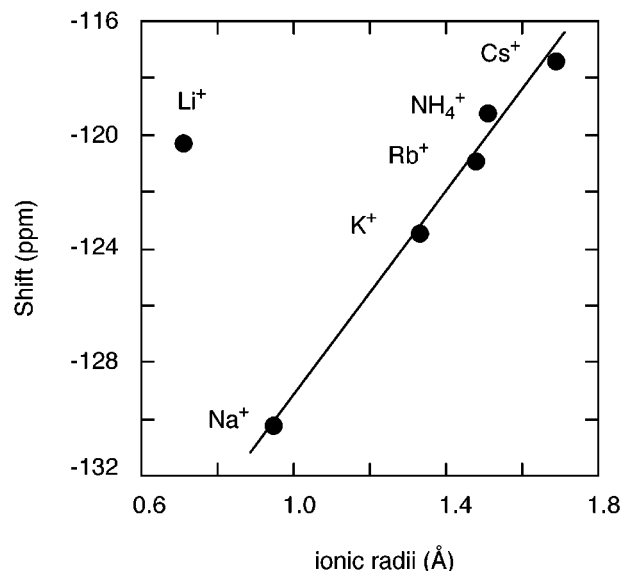
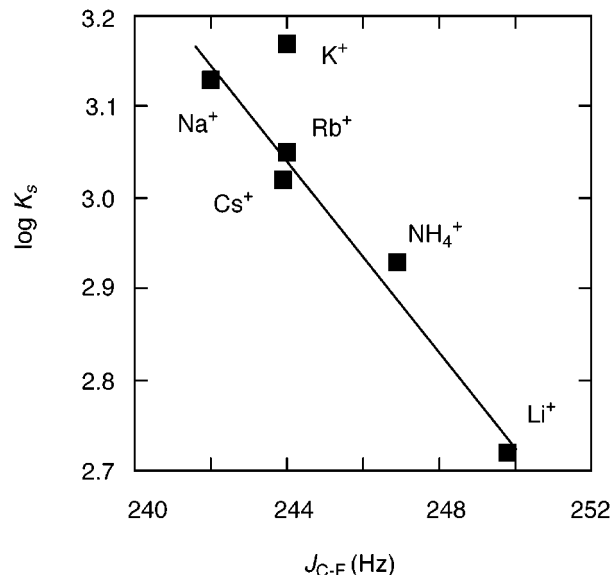
Table 3. Stability Constants of M⁺ \subset **1** and Their Spectral Features

M ⁺ \subset 1	log K _s	¹ J _{C–F} (Hz)	δ _F ^a (ppm)
metal-free 1		256.6	–116.7
Li ⁺	2.7	249.8	–112.5, –128.1
Na ⁺	3.1	242.0	–130.2
K ⁺	3.2	244.0	–123.5
Rb ⁺	3.1	244.0	–120.9
Cs ⁺	3.0	243.9	–117.4 (octet, J = 54.9 Hz)
NH ₄ ⁺	2.9	246.9	–119.3

^a Shift (ppm) from CFCl₃.

spectra in CDCl₃/CD₃CN (1/1, v/v). As described below, the spectra of the cation complexes are remarkably different from that of the metal-free **1**, and the aromatic proton signals appear at lower fields than that of the metal-free **1**. Therefore, the stability constants were easily obtained by observing the M⁺ \subset **1**/1 ratios. The reaction was very slow at 25 °C, and 2 weeks were necessary to achieve the equilibrium. The constants could not be measured by other highly accurate methods like titration because of the slow reaction rate. As shown in Table 3, cation selectivity was very small compared to the hexafluoro cage compound **4**.² This phenomenon resulted from the introduction of flexible ethyleneoxa units into the cage structure. Similar tendency was observed in the pyridine-containing cage compound **3**.³ The reactions of the fluorine-free compound **2** and metal picrates were also investigated, however, complex formation was not observed in the ¹H NMR spectra. Therefore, cations could not be captured by the four N atoms and two O atoms; four C–F units play a dominant role in the complexation. Compound **2** reacts only with an ammonium ion, but the complexation was weak. In this case, inclusion occurs by weak hydrogen bonds, NH₄⁺⋯O and NH₄⁺⋯N.

Spectroscopic Features in Complexation. The remarkable NMR spectral features during the C–F \cdots M⁺ interaction are reported, that is, (1) the ¹⁹F signal shifts to the upper field and (2) the J_{C–F} coupling constant decreases in the ¹³C NMR spectrum.^{2,12} The same phenomena were observed in the alkali metal complexes of **1**. The spectral features of the metal-free **1** and its complexes are summarized in Table 3. The coupling constants, J_{C–F}, of the complexes M⁺ \subset **1** are reduced by ca. 7–15 Hz, and the ¹⁹F signals shift to the upper fields (~13.5 ppm). Interestingly, the ionic radii of the cations and the ¹⁹F NMR chemical shift of M⁺ \subset **1** are in a good linear relationship except Li⁺. They are proportional to the interatomic distances between F and M⁺ (Figure 6); they shift to higher fields as the cations become smaller. A similar relationship was observed in the complexes, M⁺ \subset **4**.¹³ Furthermore, a linear relationship is also observed between log K_s of the complexes and coupling constants J_{C–F} in the ¹³C NMR. The more stable complexes have smaller J_{C–F} values (Figure 7). In the ¹H NMR spectra, the methylene proton signal of **1** is sharp, while the line shapes of those of the complexes strongly depend on the included cation size (Figure 8). The methylene signal coalesced by inclusion of the Li⁺ ion, and the signals split as the cation size increased. Finally,

**Figure 6.** Plots of ¹⁹F NMR shift of the complexes, M⁺ \subset **1** vs. ionic radii (Å) (CDCl₃/CD₃CN = 1/1, v/v, 25 °C).**Figure 7.** Plots of log K_s of M⁺ \subset **1** vs. J_{C–F} (Hz).

a clear split in the methylene signal is observed in the Cs⁺ complex. This phenomenon originated from the suppression of the structural mobility of the complexes. On the other hand, the spectral pattern of the aromatic proton is unchanged, but it shifts to low field due to the complexation.

Of particular interest was the ¹⁹F–¹³³Cs spin coupling observed in the ¹⁹F NMR spectrum. This is the third requirement of the C–F \cdots M⁺ interaction. As shown in Figure 9, an octet was observed in the spectrum of Cs⁺ \subset **1** (*I*(¹³³Cs) = 7/2, J = 54.9 Hz) at room temperature. An octet of the ¹⁹F signal was also observed in Cs⁺ \subset **4** at low temperatures.¹³ Only two such other examples are reported by Davidson et al., and they observed ¹⁹F–¹³³Cs spin coupling (J_{Cs–F} ≈ 58 Hz) in their fluorine-containing complexes.¹⁴ The Cs⁺ complex of the cryptand

(12) (a) Plenio, H.; Burth, D. *J. Chem. Soc., Chem. Commun.* **1994**, 2297–2298. (b) Plenio, H.; Diodone, R. *J. Am. Chem. Soc.* **1996**, *118*, 356–367. (c) Plenio, H.; Diodone, R. *Chem. Ber.* **1997**, *130*, 963–968.

(13) Takemura, H.; Nakashima, S.; Kon, N.; Inazu, T. *Tetrahedron Lett.* **2000**, *41*, 6105–6109.

(14) (a) Boyd, A. S. F.; Davidson, J. L.; McIntosh, C. H.; Leverd, P. C.; Lindsell, W. E.; Simpson, N. J. *J. Chem. Soc., Dalton Trans.* **1992**, 2531–2532. (b) Davidson, J. L.; McIntosh, C. H.; Leverd, P. C.; Lindsell, W. E.; Simpson, N. J. *J. Chem. Soc., Dalton Trans.* **1994**, 2423–2429.

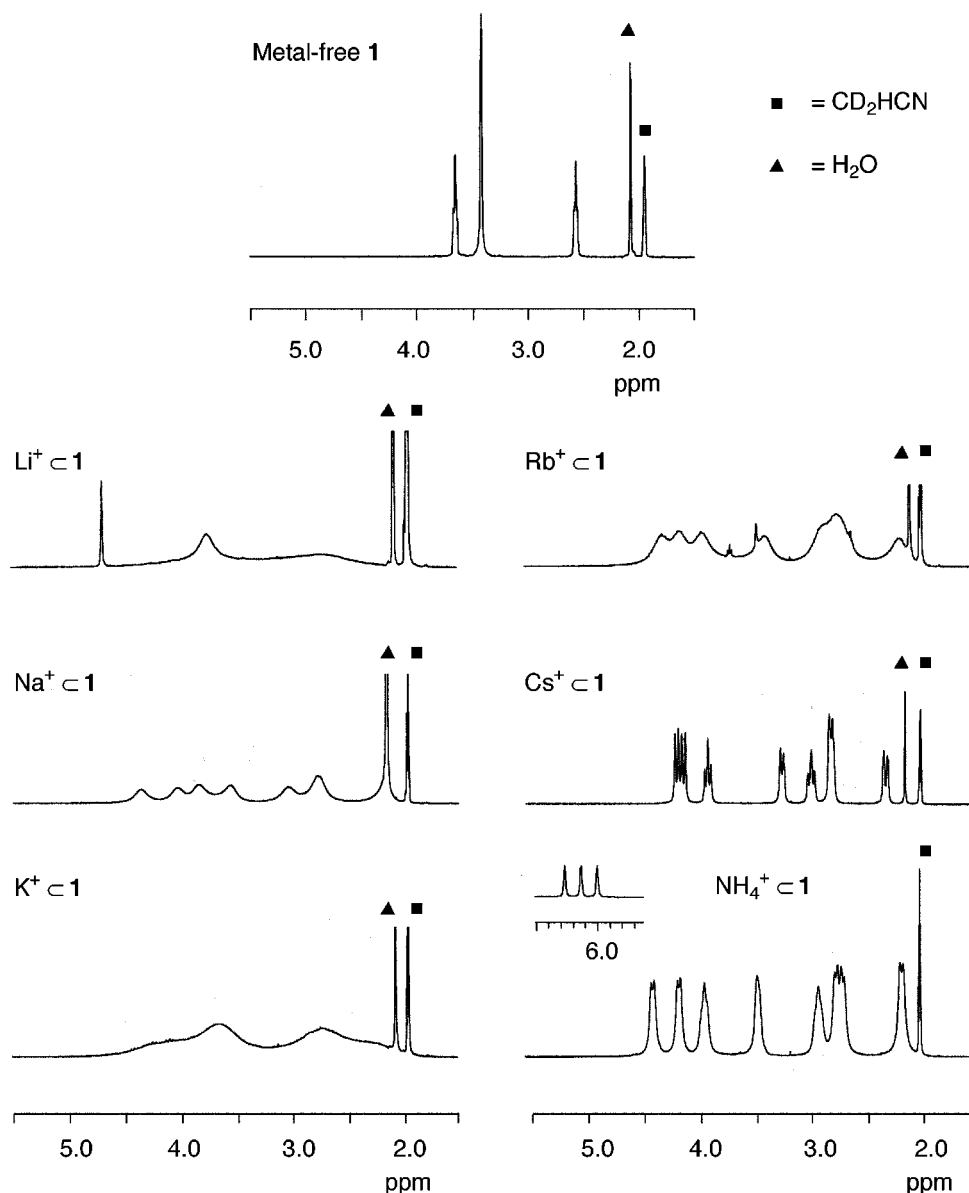


Figure 8. ^1H NMR spectra of the complexes, $\text{M}^+ \cdot \mathbf{1}$ ($\text{CDCl}_3/\text{CD}_3\text{CN} = 1/1$, v/v, 25 °C).

reported by Plenio et al. did not show the spin coupling despite the very similar structure to **1**.⁵ The ^{19}F NMR signal of the other complexes, $\text{M}^+ \cdot \mathbf{1}$ ($\text{M} = \text{Li}^+ - \text{Rb}^+$, NH_4^+), did not show this kind of spin coupling.

Conclusion

The X-ray crystallographic analyses, complex formation, and spectral changes showed that the $\text{C}-\text{F} \cdots \text{M}^+$ interaction is relatively strong. Under specific conditions in which several $\text{C}-\text{F}$ units are in an adequate arrangement, the $\text{C}-\text{F}$ unit strongly binds cations. The donor ability of $\text{C}-\text{F}$ is comparable to ether oxygen, or sometimes stronger. The specific spectral changes are observed in the ^1H , ^{13}C , and ^{19}F NMR spectra due to this interaction, and these are very important probes to detect the interaction. A dominant factor of the $\text{C}-\text{F} \cdots \text{M}^+$ interaction can be considered as a cation-dipole interaction. Nevertheless, the dative bond also cooperates in the binding of the cations because we can see remarkable NMR spectral changes and the $^{19}\text{F}-^{133}\text{Cs}$ spin coupling; there is a bond via electrons.

Experimental Section

General Procedure. Melting points were measured in N_2 sealed tubes and are uncorrected. The ^1H , ^{13}C , and ^{19}F NMR spectra were recorded at 400.1, 100.6, and 376.5 MHz, with TMS and CFCl_3 as internal references, respectively. FAB mass spectra were obtained with *m*-NBA (3-nitrobenzyl alcohol) as a matrix. Elemental analyses were performed at the Service Centre of the Elementary Analysis of Organic Compounds affiliated with the Faculty of Science, Kyushu University. All solvents and reagents were of reagent quality and used without further purification.

Cation-Free 1. The potassium complex, $\text{K}^+ \cdot \mathbf{1} \cdot \text{Br}^-$ (99.8 mg, 0.12 mmol) was dissolved in hot HCl (6 M, 15 mL) and concentrated to dryness. The residual white powder was dissolved in water, and the aqueous solution was treated with aqueous tetramethylammonium hydroxide. The resultant white precipitates were collected and recrystallized from benzene to afford colorless prisms (65.8 mg, 77.3%): mp > 294.4 °C (dec in an N_2 sealed tube); ^1H NMR (CDCl_3) δ 7.08 (t, $J = 7$ Hz, 8H), 6.91 (t, $J = 7$ Hz, 4H), 3.72 (t, $J = 6$ Hz, 8H), 3.45 (s, 16H), 2.62 (t, $J = 6$ Hz, 8H); ^{13}C NMR (CDCl_3) δ 161.77, 159.22, 130.26, 130.21, 125.87, 125.72, 120.70, 120.65, 66.94, 52.62, 52.06; ^{19}F NMR (CDCl_3) δ -117.16, -117.18, -117.20; MS (FAB, m/z) 689 ($[\text{M}^+ + 1]$, 46). Anal. Calcd for

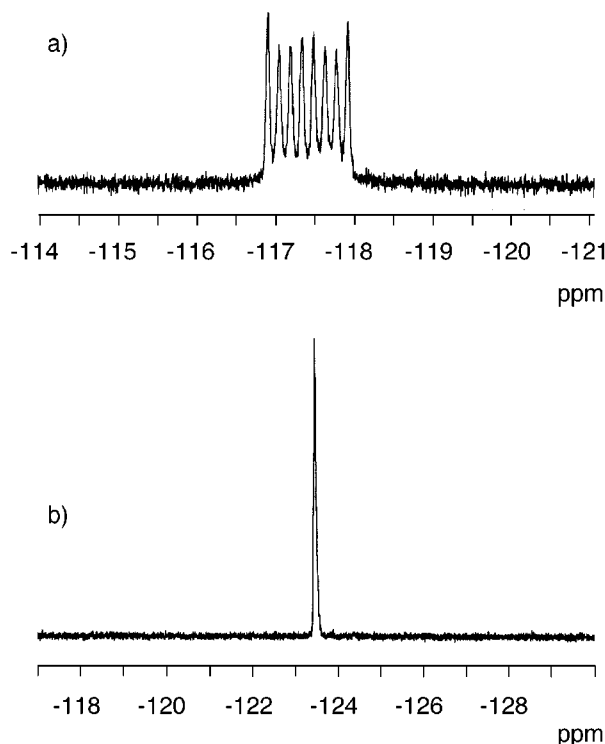


Figure 9. ^{19}F NMR spectra of (a) $\text{Cs}^+ \subset \mathbf{1}$ and (b) $\text{K}^+ \subset \mathbf{1}$.

$\text{C}_{40}\text{H}_{44}\text{N}_4\text{O}_2\text{F}_4 \cdot \text{C}_6\text{H}_6$: C, 72.04; H, 6.57; N, 7.31. Found: C, 72.00; H, 6.62; N, 7.39. The quantity of the solvent included in the analytical sample was confirmed on the basis of the ^1H NMR spectrum.

$\text{K}^+ \subset \mathbf{1} \cdot \text{Br}^-$. The data of this compound were described in ref 4a.

$\text{Cs}^+ \subset \mathbf{1} \cdot \text{Pic}^-$. Compound **1** (51.4 mg, 0.067 mmol) and cesium picrate (40.2 mg, 0.11 mmol) were dissolved in 4 mL of mixed solvent ($\text{CH}_2\text{Cl}_2/\text{CH}_3\text{CN} = 1/1$, v/v), and the solution was stirred overnight at room temperature. After removal of the solvent, the residual yellow powder was washed with a small amount of water. Recrystallization of the powder from $\text{CH}_2\text{Cl}_2\text{--CH}_3\text{CN}$ afforded yellow prisms (47.8 mg, 68.0%): mp > 279.7 °C (dec in an N_2 sealed tube); ^1H NMR ($\text{CDCl}_3/\text{CH}_3\text{CN}$, 1/1, v/v) δ 7.33–7.27 (m, 8H), 7.18 (t, $J = 7$ Hz, 4H), 4.16 (d, $J = 12$ Hz, 4H), 4.09 (d, $J = 12$ Hz, 4H), 3.87 (t, $J = 11$ Hz, 4H), 3.21 (d, $J = 12$ Hz, 4H), 2.94 (t, $J = 11$ Hz, 4H), 2.77 (d, $J = 11$ Hz, 8H), 2.28 (d, $J = 14$ Hz, 4H); ^{13}C NMR ($\text{CDCl}_3/\text{CH}_3\text{CN}$, 1/1, v/v) δ 158.90, 156.48, 132.21, 132.17, 131.69, 131.65, 125.34, 125.19, 124.95, 124.20, 124.05, 123.05, 123.02, 67.74, 54.17, 52.19, 50.63; ^{19}F NMR ($\text{CDCl}_3/\text{CH}_3\text{CN}$, 1/1, v/v) δ -117.92, -117.77, -117.63, -117.49, -117.34, -117.18, -117.04, -116.90; MS (FAB, m/z) 821 ($[\text{M} + \text{Cs}]^+$, 62). Anal. Calcd for $\text{C}_{46}\text{H}_{46}\text{N}_7\text{O}_9\text{F}_4\text{Cs}$: C, 52.63; H, 4.42; N, 9.34. Found: C, 52.90; H, 4.49; N, 9.31.

Measurements of Stability Constants. A solution of **1** in a mixture of $\text{CDCl}_3/\text{CD}_3\text{CN}$ (1/1, v/v) at a concentration of 1.05×10^{-3} M was added to the alkali metal picrates (0.51–0.77 equiv). Each mixture was allowed to stand for 2 weeks at 25 ± 0.5 °C. After the equilibrium was established, the ^1H NMR spectra were recorded and the ratios of the metal-free **1**, its complex, and picrate were calculated. The stability constants were determined on the basis of the calculated concentrations of the species using the following equation: $K = [\text{M}^+ \subset \mathbf{1}]/[\mathbf{1}][\text{M}^+\text{Pic}]$.

X-ray Crystallographic Data. Crystal data for **1**: $\text{C}_{49}\text{H}_{53}\text{N}_4\text{O}_2\text{F}_4$, $M_r = 805.98$ g mol^{-1} , colorless prismatic crystal (grown from $\text{CH}_2\text{Cl}_2\text{--C}_6\text{H}_6$ mixture), size $0.50 \times 0.30 \times 0.10$ mm, monoclinic, space group $C2/c$ (#15), $a = 37.9015(9)$ Å, $b = 11.6150(3)$ Å, $c = 19.6321(5)$ Å, $\beta = 102.1239(6)^\circ$, $V = 8449.7(4)$ Å 3 , $Z = 8$, $\rho_{\text{calcd}} = 1.267$ g cm^{-3} , $\mu(\text{Mo K}\alpha) = 0.89$ cm^{-1} , $F(000) = 3416.00$, $T = -180 \pm 1$ °C using the $\omega - 2\theta$ scan technique to a maximum 2θ value of 55.0° . A total of 39 953 reflections were collected. The final cycle of the full-matrix least-squares refinement was based on 7042 observed reflections ($I > 3.00\sigma(I)$) and 551 variable parameters and converged with unweighted and weighted agreement factors of $R = 0.039$, $R_w = 0.062$, and $\text{GOF} = 1.06$. The maximum and minimum peaks on the final difference Fourier map corresponded to 0.54 and -0.37 $\text{e}^-/\text{Å}^3$, respectively.

Crystal data for $\text{K}^+ \subset \mathbf{1} \cdot \text{Br}^-$: $\text{C}_{42}\text{H}_{50}\text{N}_4\text{O}_4\text{F}_4\text{KBr}$, $M_r = 869.88$ g mol^{-1} , colorless prismatic crystal (grown from $\text{CH}_2\text{Cl}_2\text{--MeOH}$ mixture), size $0.50 \times 0.30 \times 0.50$ mm, monoclinic, space group $C2/c$ (#15), $a = 19.550(2)$ Å, $b = 20.356(1)$ Å, $c = 12.5090(7)$ Å, $\beta = 125.814(3)^\circ$, $V = 4036.8(5)$ Å 3 , $Z = 4$, $\rho_{\text{calcd}} = 1.431$ g cm^{-3} , $\mu(\text{Mo K}\alpha) = 11.90$ cm^{-1} , $F(000) = 1808.00$, $T = -180 \pm 1$ °C using the $\omega - 2\theta$ scan technique to a maximum 2θ value of 55.0° . A total of 18 274 reflections were collected. The final cycle of the full-matrix least-squares refinement was based on 2725 observed reflections ($I > 3.30\sigma(I)$) and 265 variable parameters and converged with unweighted and weighted agreement factors of $R = 0.056$, $R_w = 0.105$, and $\text{GOF} = 1.42$. The maximum and minimum peaks on the final difference Fourier map corresponded to 0.75 and -0.57 $\text{e}^-/\text{Å}^3$, respectively.

Crystal data for $\text{Cs}^+ \subset \mathbf{1} \cdot \text{Pic}^-$: $\text{C}_{46}\text{H}_{46}\text{N}_7\text{O}_9\text{F}_4\text{Cs}$, $M_r = 1049.81$ g mol^{-1} , yellow prismatic crystal (grown from $\text{CH}_2\text{Cl}_2\text{--CH}_3\text{CN}$ mixture), size $0.50 \times 0.50 \times 0.50$ mm, monoclinic, space group $C2/c$ (#15), $a = 20.8442(7)$ Å, $b = 20.0963(5)$ Å, $c = 12.6628(4)$ Å, $\beta = 123.8475(7)^\circ$, $V = 4405.4(2)$ Å 3 , $Z = 4$, $\rho_{\text{calc.}} = 1.583$ g cm^{-3} , $\mu(\text{Mo K}\alpha) = 9.24$ cm^{-1} , $F(000) = 2136.00$, $T = -180 \pm 1$ °C using the $\omega - 2\theta$ scan technique to a maximum 2θ value of 55.0° . A total of 20 332 reflections were collected. The final cycle of the full-matrix least-squares refinement (SHELXL-97) was based on 4873 observed reflections ($I > 2.00\sigma(I)$) and 442 variable parameters and converged with unweighted and weighted agreement factors of $R = 0.027$, $R_w = 0.082$, and $\text{GOF} = 1.23$. The maximum and minimum peaks on the final difference Fourier map corresponded to 0.57 and -0.82 $\text{e}^-/\text{Å}^3$, respectively.

Crystallographic data (excluding structure factors) for the structures reported in this paper have been deposited with the Cambridge Crystallographic Data Centre as supplementary publication no. CCDC 149141 for **1**, 149142 for $\text{K}^+ \subset \mathbf{1}$, and CCDC 149143 for $\text{Cs}^+ \subset \mathbf{1}$. Copies of the data can be obtained free of charge upon application to CCDC, 12 Union Road, Cambridge CB2 1EZ, U.K. [Fax: +44(1223)336-033; E-mail: deposit@ccdc.cam.ac.uk].

Acknowledgment. This research was supported by a Grant-in-Aid for Developmental Scientific Research provided by the Ministry of Education, Science, Sports and Culture, Japan (No. 12640522) and for COE Research "Design and Control of Advanced Molecular Assembly Systems" from the Ministry of Education, Science, Sports and Culture, Japan (No. 08CE2005). The author thanks Professor Emeritus I. D. Brown for his kind comments on the discussion of bond-valence sum.

JO0016778